The metallicity dependence of WR wind models

G. Gräfener & W.-R. Hamann

Department of Physics, University of Potsdam, Germany

Abstract. With the advance of stellar atmosphere modelling during the last few years, large progress in the understanding of Wolf-Rayet (WR) mass loss has been achieved. In the present review we give an overview of the most recent developments, including our own results from hydrodynamic non-LTE model atmospheres. In particular, we address the important question of the Z-dependence of WR mass loss. We demonstrate that the current models for radiatively driven winds imply a rather strong dependence on Z. Moreover, we point out the key role of the L/M-ratio for WR-type mass loss.

1. WR-type stellar winds

WR stars show exceptionally strong winds with mass loss rates of the order of the single scattering limit or above. The observed wind efficiency numbers $\eta = \dot{M} v_\infty / (L_\star / c)$, which denote the ratio between the wind momentum and the momentum of the radiation field, are typically in the range of 1-5. Therefore, *if* WR-type winds are driven by radiation, photons must be used more than once, i.e., after absorption photons must either be re-distributed into different wavelength regimes or they must be scattered more than once by overlapping lines in the extended wind. Because of their high wind densities, WR stars develop extended atmospheres where the hydrostatic layers are completely hidden to the observer. In combination with their extremely hard radiation fields, they develop extreme non-LTE conditions that require sophisticated modeling techniques.

The key question concerning WR mass loss is *why* a star becomes a Wolf-Rayet star. The observed parameters of early-type O stars, namely their luminosities and effective temperatures, are in principle comparable with late-type WN stars. O supergiants even tend to show a similar He- and N-enriched surface composition. Because of their higher mass loss rates, however, WR stars show dramatically different spectra with strong and broad wind emissions where O stars show tiny photospheric absorption lines.

If the WR winds are radiation-driven like OB star winds, one would also expect a similar Z-dependence of their mass loss. In this case, however, the question must be addressed why WNL stars are so different from O stars.

2. Monte-Carlo models

The first wind models which were able to reproduce the high efficiency factors of WR winds, were obtained by Monte-Carlo techniques (Lucy & Abbott 1993; Springmann 1994). In this approach the path of single photon energy packets, released at the wind base, is followed until they escape from the wind. On their way through the wind, the photons are scattered by Doppler-shifted spectral lines which are treated as infinitely narrow pure scattering opacities. For each scattering process the energy is determined which is transferred from the radiation field to the wind material or vice versa. Finally a 'global' solution for the mass loss rate is obtained by comparing the total mechanical wind energy which is gained from the radiation field per time interval with the overall wind luminosity $\dot{M}v_\infty^2$. In the approach of Lucy & Abbott (1993) the line opacities are taken from a line list and the atomic populations and ionization are calculated in a modified nebular approximation. Springmann (1994), on the other hand, used a purely statistical approach for the strength and the distribution of the line opacities.

The pilot studies by Lucy & Abbott (1993) and Springmann (1994) showed that high wind momenta with η up to 10 can in principle be achieved by multiple line scattering if enough line opacities are present. Nevertheless, these models do not explain *why* the WR mass loss rates are so high. They rely on an adopted *beta*-type velocity structure with a *prescribed* terminal wind velocity v_∞ (note that the wind luminosity goes with v_∞^2). In particular, the models significantly underestimate the wind acceleration in the deeper atmospheric layers below a radius of $\sim 2\,R_\star$.

Recently Vink & de Koter (2005, see also this volume) investigated the Z-dependence of WR mass loss by means of similar models as Lucy & Abbott (1993). In their approach, however, the excitation temperatures which enter the calculation of the ionization structure and the atomic populations, are extracted from a grid of model atmospheres (see Vink et al. 1999). For the example of a late-type WN star Vink & de Koter find a similar Z-dependence as for O-stars with $\dot{M} \propto Z^{0.86}$ which *flattens* at metallicities below $10^{-4}Z_\odot$ because the line driving is taken over by N and He. Note that the mass loss rates at this metallicity are so small ($\sim 10^{-7}M_\odot/\mathrm{yr}$) that the star would not be identified as a WR-type from its spectral appearance. For a WCL model they find a relation with $Z^{0.66}$ which flattens already at $10^{-3}Z_\odot$.

3. Optically thick wind models

A completely complementary approach to the previous one is the critical-point analysis for optically thick winds (e.g. Pistinner & Eichler 1995; Nugis & Lamers 2002). The underlying assumption of this method is that, because of their high mass loss rates, WR atmospheres are so extended that the sonic point of the wind flow is located at large flux-mean optical depth τ_s. If τ_s is large enough the radiation transport can be treated in the diffusion limit. The expression for the radiative acceleration then simplifies to

$$a_\mathrm{rad} = \frac{1}{c}\int \chi_\nu F_\nu \mathrm{d}\nu \equiv \chi_\mathrm{Ross}\frac{L_\star}{4\pi r^2 c} \tag{1}$$

where χ_Ross denotes the Rosseland mean opacity which can easily be obtained e.g. from the OPAL opacity tables (Iglesias & Rogers 1996). This expression for a_rad is not only easy to evaluate, it also changes the dynamic wind properties

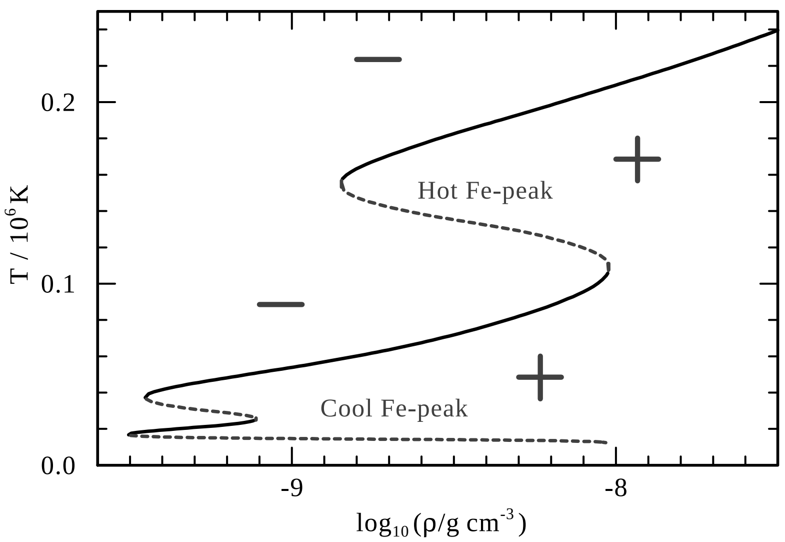

Figure 1. Solution of Eq. (5) in the ρ-T plane. The sonic-point conditions for an optically thick wind, i.e. $\chi_{\rm Ross} = \chi_{\rm crit}$ with *outward increasing* $\chi_{\rm Ross}$, are fulfilled on the solid curves between 40 and 100 kK, and above 160 kK. The Rosseland opacities in this plot are taken from the OPAL opacity tables. Typical WC star parameters are assumed.

in relation to OB stars. The wind acceleration in a spherically expanding radiatively driven flow is given by the contributions of the gravitational attraction, the pressure gradient, and the radiative acceleration

$$v\frac{\mathrm{d}v}{\mathrm{d}r} = -\frac{MG}{r^2} - \frac{1}{\rho}\frac{\mathrm{d}p}{\mathrm{d}r} + a_{\rm rad}. \tag{2}$$

When the velocity gradient is extracted from the pressure gradient this equation becomes

$$\left(v - \frac{a^2}{v}\right)\frac{\mathrm{d}v}{\mathrm{d}r} = -\frac{MG}{r^2} + 2\frac{a^2}{r} - \frac{\mathrm{d}a^2}{\mathrm{d}r} + a_{\rm rad} \tag{3}$$

where a denotes the sonic speed. In the diffusion limit $a_{\rm rad}$ does not depend on $\frac{\mathrm{d}v}{\mathrm{d}r}$. Eq. (3) then has a critical point at the sonic radius $r_{\rm s}$ where $v = a$. A finite value of $\frac{\mathrm{d}v}{\mathrm{d}r}$ can only be obtained if the right hand side of Eq. (3) is zero at this point.

$$0 = -\frac{MG}{r_{\rm s}^2} + 2\frac{a^2}{r_{\rm s}} - \frac{\mathrm{d}a^2}{\mathrm{d}r_{\rm s}} + a_{\rm rad} \tag{4}$$

Note that for the thin winds of OB stars $a_{\rm rad}$ depends on $\frac{\mathrm{d}v}{\mathrm{d}r}$ via Doppler shifts. The critical point of Eq. (3) is then located at a significantly higher speed (the so-called Abbott speed) which corresponds to the fast radiative-acoustic wave mode (Abbott 1980). For optically thick winds Eq. (4) serves as a limiting condition for the mass loss rate. For reasonable wind parameters the second and third term on the right hand side of Eq. (4) become negligible so that

$$\frac{MG}{r_{\rm s}^2} \approx a_{\rm rad}(r_{\rm s}) \equiv \chi_{\rm crit}\frac{L_\star}{4\pi r_{\rm s}^2 c}. \tag{5}$$

The Eddington limit, referring to the Rosseland mean opacity, is therefore crossed at the sonic point. The critical value $\chi_{\rm crit}$ for the Rosseland mean opacity can be calculated directly from the given L/M ratio for a specific object.

In Fig. 1 we plot the the solution of Eq. (5), i.e. the region in density- temperature space where $\chi_{\rm Ross}(\rho, T) = \chi_{\rm crit}$, for the example of a typical WC star. In a stable configuration the radiative force in the hydrostatic layers, below $r_{\rm s}$, must be lower than the Eddington value. $\chi_{\rm Ross}$ therefore has to increase outward, with decreasing density. As shown in Fig. 1 this condition is fulfilled at the hot edges of the two Fe opacity peaks, at temperatures in the range of 40–100 kK and above 160 kK. The resulting mass loss rates on these two curves are given by $\dot{M} = 4\pi R_\star^2 \rho\, a$ where the sonic speed a depends on T and the chemical composition of the wind material.

To estimate the actual density and temperature at the sonic point, however, a further constraint is needed. At this point Nugis & Lamers (2002) utilize an approximate relation between temperature and optical depth by Lucy (1971)

$$T^4(r) = \frac{3}{4} T_{\rm eff}^4 \left(\tau'(r) + \frac{4}{3} W(r) \right) \tag{6}$$

with the modified optical depth τ' and the dilution factor W which is close to one in our case. τ' is obtained from the assumption that the outer wind is driven by radiation. For this purpose it is necessary to take the density and velocity structure above the sonic point into account. Again, the results rely on the adopted velocity distribution $v(r)$, where a β-type velocity law with a terminal wind velocity in the observed range of 1000–3000 km/s is used.

The analysis by Nugis & Lamers reveals important insights how the mass loss of WR stars might be adjusted. They find that the observed WR mass loss rates are in agreement with the optically thick wind assumption, with two distinct sonic-point temperature regimes. The cool regime with typical $T_{\rm s}$ in the range of 40–100 kK and $\tau_{\rm s} = 3 - 10$ is related to late-type WN stars and the hot regime with $T_{\rm s} \approx 160$ kK and $\tau_{\rm s} = 1 - 30$ to early-type WN and WC stars. For the Z-dependence of early-type WN stars Nugis (these proceedings) finds very steep exponents in the range 1-1.5, dependent on the stellar mass. When the mass loss goes down at low metallicities the validity of the optically thick wind assumption might however be questionable.

4. PoWR hydrodynamic model atmospheres

From Monte-Carlo models we have learned that the acceleration of the outer part of WR winds, namely their high wind performance numbers, can in principle be explained by multiple scattering processes. In addition, the critical-point analysis by Nugis & Lamers revealed that the mass loss rates are presumably adjusted by the radiative driving of Fe-peak opacities at large optical depth. As a consequence we expect two regimes of WR mass loss corresponding to the two Fe-opacity peaks at cool and hot temperatures. Moreover, in addition to a Z-dependence, we expect a strong dependence of WR mass loss on the L/M ratio.

Regardless of these important findings, fundamental questions still remain open. All of the previous models rely on pre-defined velocity distributions $v(r)$.

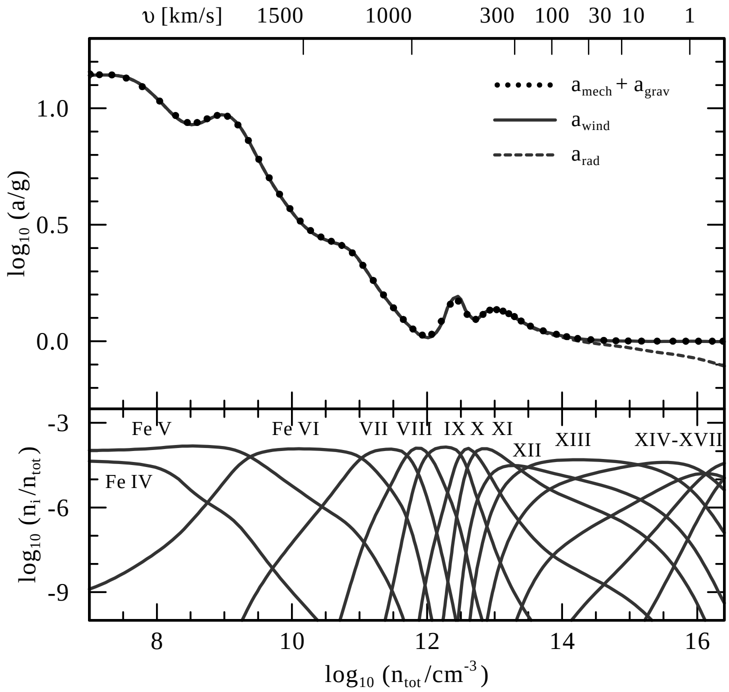

Figure 2. Top: Acceleration within our hydrodynamic WC star model in units of the local gravity. The wind acceleration $a_{\rm wind}$ due to radiation + gas pressure is in precise agreement with the mechanical + gravitational acceleration $a_{\rm mech} + a_{\rm grav}$. Bottom: Fe-ionization structure.

It is therefore not clear if the high mass loss rates can be maintained throughout the *whole* wind by radiation pressure alone. In reality, the terminal wind velocity adjusts by an interplay between the acceleration in the outer parts of the wind and the limiting condition at the critical point. Moreover, the optically thick wind assumption, i.e., the question whether the diffusion limit is valid at the critical point or if the radiation field is affected by Doppler shifts, remains to be verified. Finally, spectral analyses and time resolved spectroscopy show direct evidence for a clumped wind structure, but the effects of clumping are not included in any previous stellar wind models.

The new Potsdam Wolf-Rayet (PoWR) hydrodynamic model atmospheres (see Gräfener & Hamann 2005; Hamann & Gräfener 2003; Koesterke et al. 2002; Gräfener et al. 2002) address exactly the questions explained above. By a combination of line-blanketed non-LTE model atmospheres with the equations of hydrodynamics, Gräfener & Hamann (2005) obtained the first fully self-consistent models for WR winds. In these models $\dot{M}$, $v(r)$, $T(r)$, and the full set of non-LTE population numbers are computed consistently with the radiation field in the comoving frame (CMF), i.e., the radiation transport, the equations of statistical equilibrium, the energy equation, and the equation of motion are simultaneously solved. Through the exact solution of the radiation transport no simplifying assumptions concerning the radiative acceleration are necessary. $a_{\rm rad}$ is simply

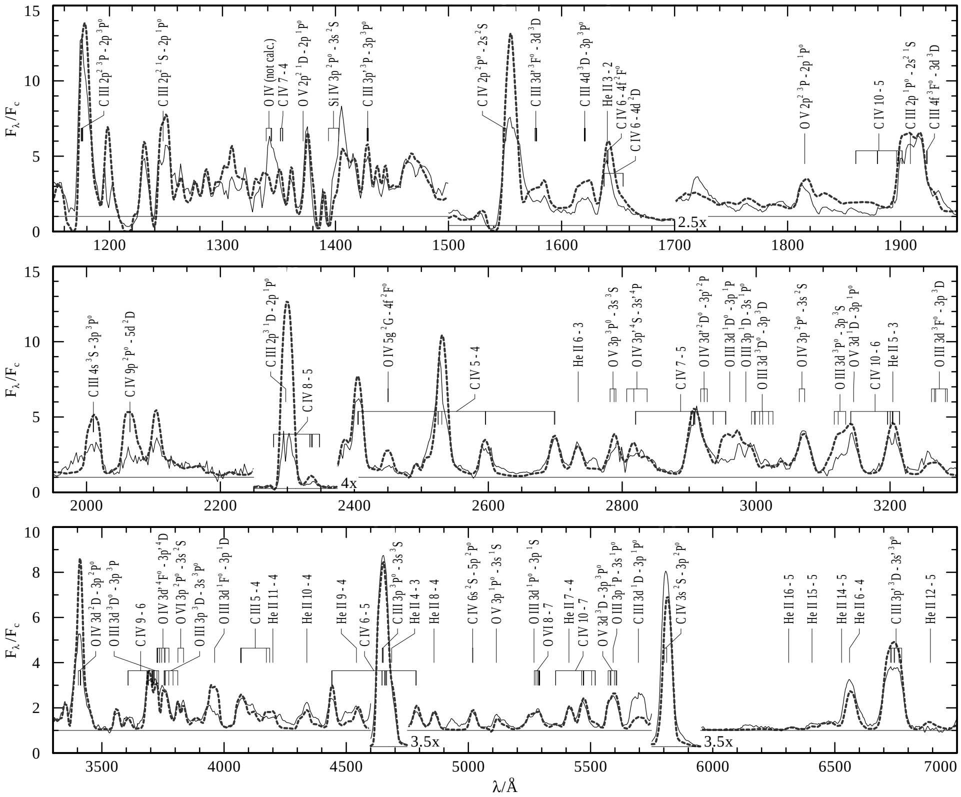

Figure 3. WR 111: Comparison of the synthetic spectrum from our hydrodynamic 13.6 $M_{\odot}$ WCE model (dashed line, grey) with observations.

calculated by integrating the product of opacity and flux over frequency (see Eq. 1), which are both given on a fine frequency grid in the co-moving frame of reference. Moreover, clumping is taken into account in the limit of optically thin clumps. The resultant models describe the conditions in WR atmospheres correctly, and provide synthetic spectra, i.e., they allow a direct comparison with observational material. Nevertheless, simplifying assumptions are still necessary. These are especially the assumption of a constant Doppler broadening velocity throughout the atmosphere and the omission of opacities, partly due to the neglect of trace elements like Ne, Ar, S, or P and partly due to incompleteness of the available data.

In the following we present PoWR models for both expected temperature regimes. 'Hot' models with core temperatures of $T_{\star} = 140\,\mathrm{kK}$ for early-type WC stars on the He-main sequence, and 'cool' models for late-type WN stars in the range of $T_{\star} = 30$–$60\,\mathrm{kK}$. For the latter we also investigate the detailed Z-dependence.

4.1. Hot objects: early-type WC stars

WC stars are expected to be chemically homogeneous stars in the phase of central He-burning. Because of their strong mass loss they show exceptionally

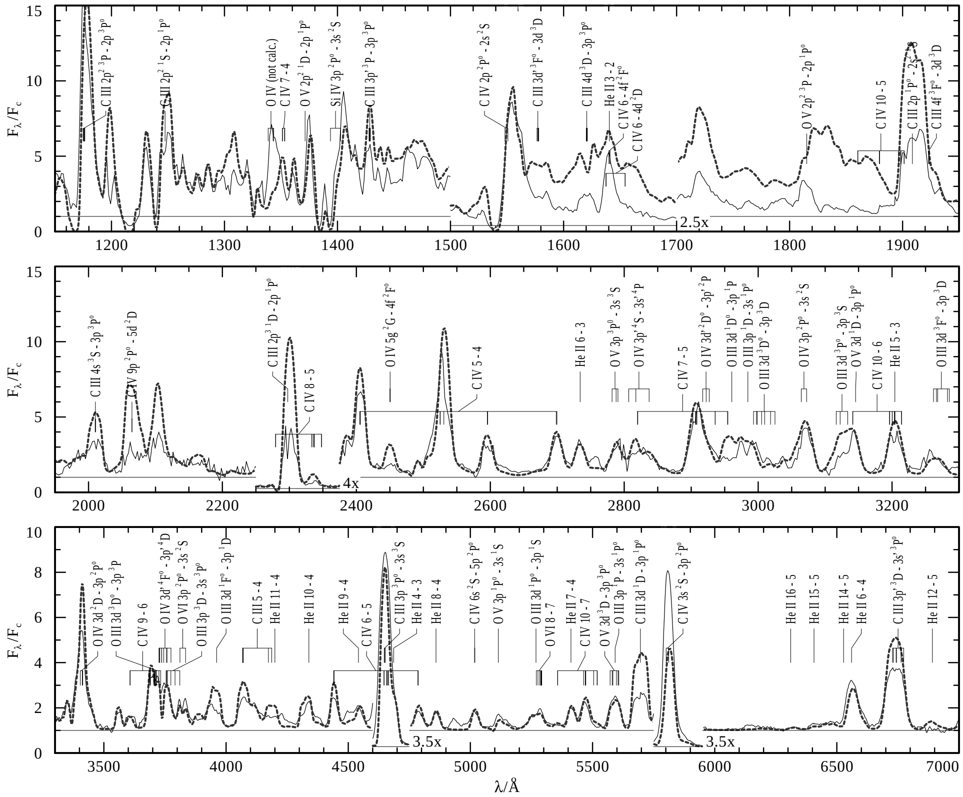

Figure 4. Same as Fig. 3, but a reduced mass of $12\,M_\odot$ has been adopted in the hydrodynamic calculation.

strong emission lines of He, C and O. They are an ideal target for our model calculations because they obey a mass-luminosity relation which has been derived theoretically e.g. by Langer (1989). This means that the number of free parameters in our calculation is reduced by one. When the luminosity and the chemical composition for a specific object are given, e.g. from spectral analyses, only the stellar core radius $R_\star$ or, equivalently, the corresponding effective core temperature $T_\star$ remains. In fact, this parameter is also given by spectral analyses. There are, however, striking discrepancies between the observed $T_\star$ (50–90 kK) and the theoretically expected core temperatures from stellar structure calculations (120–150 kK).

There are in principle two ways how this discrepancy might be resolved. First, due to their strong winds, the WC star atmospheres are so extended (*above* the sonic point) that the photosphere is located far out in the wind (at $\sim 3\,R_\star$). The hydrostatic layers are therefore not directly observable. Second, He-burning stars might develop an extended convective envelope *below* the sonic point. Based on static models, Ishii et al. (1999) have shown that this might be the case for very high luminosities and/or metallicities. Note, however, that the extension in these models occurs when the Eddington limit is approached close to the 'hot' Fe-opacity peak. Presumably because of the hydrostatic assumption, these models form an extended convective zone instead of launching an optically thick wind. Our hydrodynamic wind models now have the potential to discriminate between these two possibilities. On one hand they provide the sub-photospheric wind structure, on the other hand they can show under which conditions an optically thick wind actually develops.

The first self-consistent PoWR wind models for an early-type WC star are described in Gräfener & Hamann (2005). These calculations are based on a previous spectral analysis of the WC 5 prototype WR 111 (Gräfener et al. 2002), where an effective core temperature of $T_\star = 85\,\mathrm{kK}$ was obtained. For the wind calculations, the models had to be extended by the Fe-peak opacities, namely the Fe M-shell ions Fe IX–XVII. First tests, however, demonstrated that *no wind-driving is possible for 'cool' stellar temperatures around 85 kK.* The models in this temperature regime showed a strong deficiency in the radiative acceleration directly above the sonic point. If, on the other hand, $T_\star$ is increased to a value of 140 kK (at fixed luminosity) this problem is resolved.

Remaining problems in intermediate wind layers (at velocities around 1000 km/s) are compensated by the choice of a relatively high clumping factor ($D = 50$). Wind clumping reduces the *observed* mass loss rates by a factor of $\sqrt{D}$ because it enhances recombination processes. When the wind density is reduced by this factor, the typical WR emission line spectrum remains constant. Our models now show that the radiative force behaves similar, i.e., when clumping is increased and $\dot{M}$ decreased the *force* remains similar which means that $a_{\rm rad}$ *increases*. Note that Gräfener & Hamann (2003) have shown that O star winds show the same behavior.

For the hydrodynamic calculations we assume a stellar mass of $13.6\,M_\odot$ according to the relation by Langer (1989) for a luminosity of $L_\star = 10^{5.45}\,L_\odot$. The resulting wind acceleration is plotted in Fig. 2 together with the Fe-ionization structure. With the obtained mass loss rate of $\dot{M} = 10^{-5.14}\,M_\odot/\mathrm{yr}$ and the terminal wind velocity of $v_\infty = 2010\,\mathrm{km/s}$ the observed spectrum of WR 111 is convincingly reproduced (Fig. 3). Nevertheless, the weakness of the electron scattering wings (e.g. of C IV 5808) indicates that the choice of $D = 50$ is too high. Although the clumping factors can only be determined very roughly, WC stars usually show values of the order of $D = 10$. Our models might therefore underestimate the mass loss rate by a factor of $\sqrt{5}$.

Concerning the temperature regime where the sonic point is located, our models are in line with the results of Nugis & Lamers (2002). However, because of the higher effective core temperature in our model, the temperature of $T_{\rm s} = 199\,\mathrm{kK}$ is already reached at smaller optical depth $\tau_{\rm s} = 5.4$ (cf. Eq. 6). Furthermore, our models show an extreme sensitivity to the L/M ratio. A change of the stellar mass from 13.6 to $12\,M_\odot$ increases the mass loss by a factor 1.5. As shown in Fig. refspec2, the resulting model spectrum the corresponds to a later spectral type.

4.2. Cool objects: WNL stars

Hamann et. al (this volume) have analyzed a large part of the galactic WN stars by means of a grid of line-blanketed PoWR models (Hamann & Gräfener 2004). The stars in this sample divide into two distinct groups. The first group consists of a mixture of early- to intermediate-type WN stars with luminosities

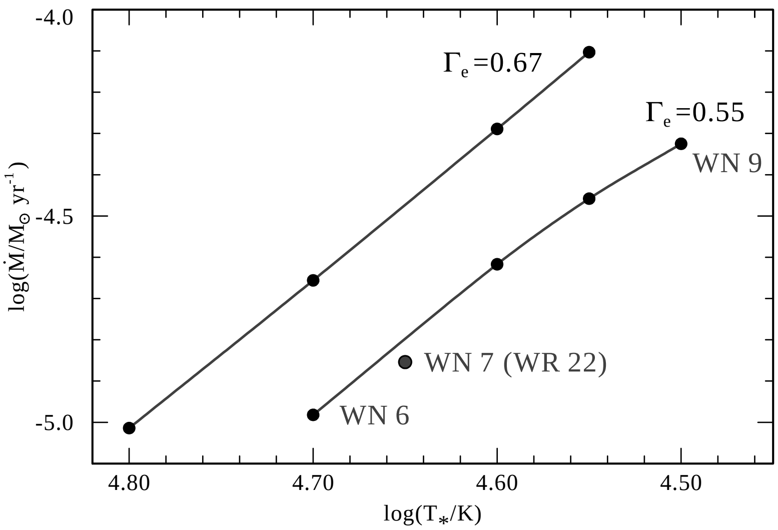

Figure 5. WNL mass loss rates for different stellar temperatures and masses (indicated by the Eddington factor $\Gamma_{\rm e}$). The model for WR 22 is calculated with an enhanced Hydrogen abundance (see text).

below $10^6\,L_\odot$. The second group consists of late-type WN stars (WN 6–9) with luminosities above $10^6\,L_\odot$. The latter are located to the right of the main sequence (at $T_\star = 35$–55 kK) and show hydrogen at their surface. The extreme brightness of these stars already implies high L/M ratios. We have therefore calculated a grid of WNL models with a fixed luminosity of $10^{6.3}\,L_\odot$ and core temperatures in the range of 30–60 kK. For the stellar masses, values of 67 and $55\,M_\odot$ were adopted, corresponding to Eddington factors $\Gamma_{\rm e} \equiv \chi_{\rm e} L_\star / 4\pi c G M_\star$ of 0.55 and 0.67. Typical WR surface abundances of $X_{\rm H} = 0.2$ and $X_{\rm N} = 0.015$, and a clumping factor of $D = 10$ are assumed.

The resulting mass loss rates are plotted in Fig. 5. As expected for optically thick winds, the mass loss shows a strong dependence on the ratio L/M or equivalently on $\Gamma_{\rm e}$. Moreover, the mass loss increases with decreasing $T_\star$, which can also be understood in the framework of the optically thick wind theory. At cooler $T_{\rm eff}$ a higher optical depths is needed at the sonic point to reach the demanded temperatures (see Eq. 6). Therefore higher wind densities are needed. The obtained synthetic spectra reflect the observed sequence of WNL spectral types, starting with WN 6 for the hot models at 55 kK to WN 9 at 31 kK.

To verify our assumption of a high L/M ratio for WNL stars we have performed more detailed investigation of the WN 7 component in the eclipsing WR+O system WR 22. The O star in this system is so faint that the flux distribution in the optical and the UV is dominated by the WR star. Nevertheless, mass estimates are available from orbital solutions for the marginally visible O star absorption features. Schweickhardt et al. (1999) and Rauw et al. (1996) have determined a mass ratio $M_{\rm WR}/M_{\rm O} = 2.7$ and values of $M_{\rm WR} \sin^3 i = 55 \pm 7\,M_\odot$ and $72 \pm 3\,M_\odot$ respectively.

With our self-consistent wind models we obtain a reasonable spectral fit for WR 22 with $\Gamma_e = 0.67$, a slightly enhanced hydrogen abundance $X_H = 0.4$, and

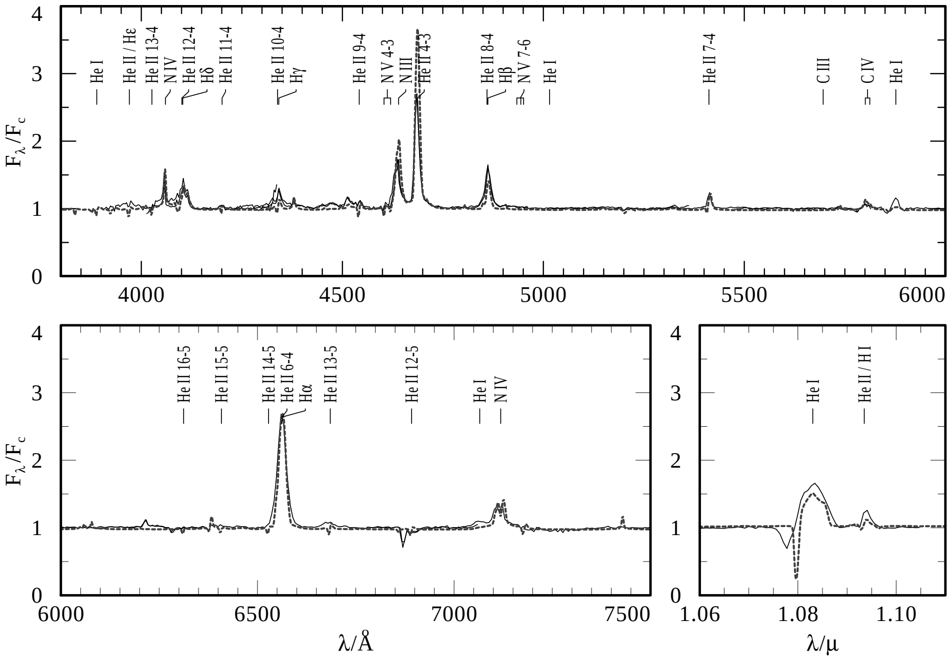

Figure 6. WR 22: Comparison of the synthetic spectrum from our hydrodynamic model (dashed line, grey) with observations.

a stellar temperature of 45 kK (see Fig.6). With the standard distance modulus of 12.1 mag to Car OB1, our model with $L_\star = 10^{6.3}\,L_\odot$ exactly reproduces the observed flux distribution. The corresponding stellar mass of $78\,M_\odot$ is in excellent agreement with the mass determination by Rauw et al. (1996). Note, however, that the resulting stellar mass depends on X_H (because Γ_e depends on X_H) *and* on the exact stellar luminosity, i.e. the adopted distance. With a distance modulus of 12.55 mag, as determined by Massey & Johnson (1993) for the Carina OB clusters Tr 14 and Tr 16, we would obtain an even higher luminosity and therefore an even higher L/M ratio. In any case, WR 22 has a luminosity equal or above $10^{6.3}\,L_\odot$ and is located rather close to the Eddington limit.

4.3. WNL stars: Z-dependence

The WR-type winds in our previous models are predominantly driven by radiation pressure on Iron line opacities. We therefore expect a strong dependence of WR mass loss on Z. To investigate this dependence we have prepared a model grid for late-type WN stars which is based on our model for WR 22. Because we already know about the importance of the L/M ratio, we have varied the Eddington factor Γ_e (or equivalently the stellar mass) in addition to the metallicity Z (note that we scale all metals *including Nitrogen* with Z). As shown in Fig.7, our models indeed show a strong Z-dependence. For models with *fixed stellar mass* we find rather similar exponents as Vink & de Koter (2005) ($\dot{M} \propto Z^{0.86}$). In addition, however, our models show a strong dependence on Γ_e. In particular, we find that optically thick winds with high WR-type mass loss rates *can also*

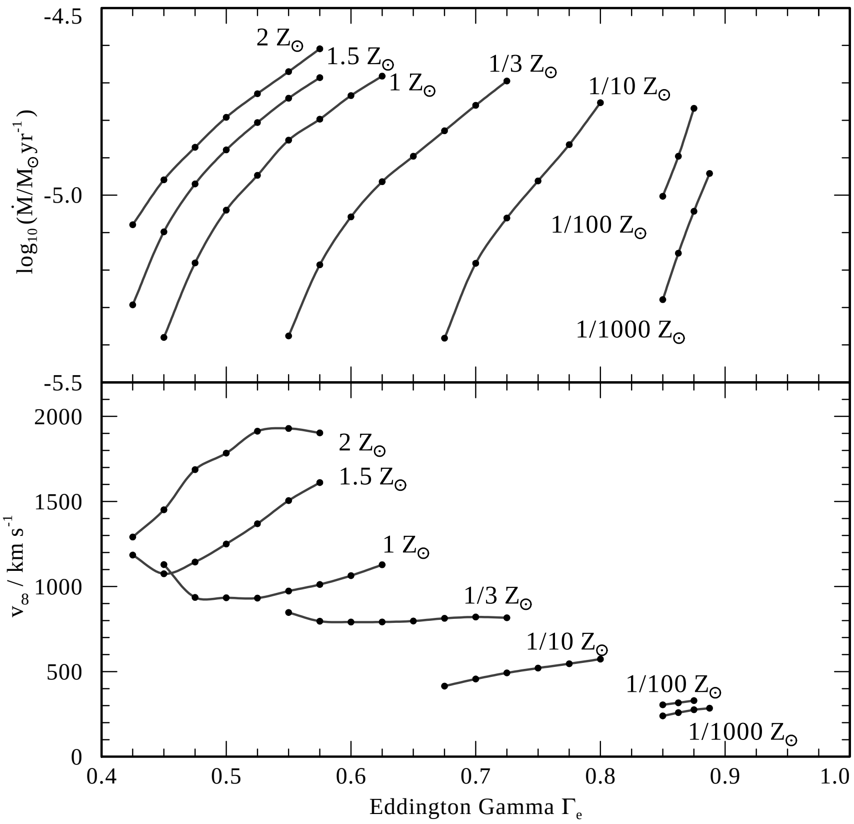

Figure 7. Z-dependence for WNL stars: Mass loss rates (top) and terminal wind velocities (bottom) as obtained from our grid of hydrodynamic models.

be maintained at extremely low Z, if the star manages to come close enough to the Eddington limit.

The obtained terminal wind velocities (Fig.7, bottom). First, our models clearly predict decreasing wind velocities with decreasing Z. This finding is generally confirmed by observations (e.g. by Conti et al. 1989), although the observational evidence is not as clear as our prediction. Moreover, our models show a rather striking behavior because the terminal velocities stay constant, or even increase with increasing mass loss rate. Obviously, our dense wind models violate the well-known wind momentum-luminosity relation for OB star winds (e.g. Kudritzki et al. 1999), which would imply $\dot{M}v_\infty = const.$ Only at the lowest densities the terminal wind velocity starts to increase as expected. A closer inspection of the models shows that the changes at high wind densities are related to changes in the ionization structure. It therefore seems that the velocity structure is dictated by ionization effects rather than a CAK-type wind physics. This is in line with our result that, in contrast to standard assumptions, the *effective* force multiplier parameter α shows values close to zero in our WC star model (see Gräfener & Hamann 2005). Also the present WNL models show a tendency towards low α-values (≈ 0.2), although not as severe as our WC model.

5. Conclusions

We want to conclude that models for radiatively driven winds imply a strong Z-dependence of WR mass loss. In addition, however, the L/M-ratio turns out to be at least equally important. Proximity to the Eddington-limit, or over-luminosity, might even be a pre-requisite for WR-type mass loss. This would naturally explain why He-burning stars *and* extremely luminous stars tend to show WR spectra. Moreover it implies an important role of rotation (which is not yet included in our models). First, rotation enhances the L/M ratio in the H-burning phase by mixing Hydrogen into the stellar core. Second, rotation reduces the effective gravity at the stellar surface and thereby also the effective Eddington factor. Finally, we want to remark that the *qualitative* behavior of WR mass loss is very well described by the theory of optically thick winds.

References

Abbott, D. C. 1980, ApJ, 242, 1183
Conti, P. S., Garmany, C. D., & Massey, P. 1989, ApJ, 341, 113
Gräfener, G. & Hamann, W.-R. 2003, in IAU Symp., Vol. 212, A Massive Star Odyssey: From Main Sequence to Supernova, ed. K. A. van der Hucht, A. Herrero, & E. César (San Francisco: ASP), 190
Gräfener, G. & Hamann, W.-R. 2005, A&A, 432, 633
Gräfener, G., Koesterke, L., & Hamann, W.-R. 2002, A&A, 387, 244
Hamann, W.-R. & Gräfener, G. 2003, A&A, 410, 993
Hamann, W.-R. & Gräfener, G. 2004, A&A, 427, 697
Iglesias, C. A. & Rogers, F. J. 1996, ApJ, 464, 943
Ishii, M., Ueno, M., & Kato, M. 1999, PASJ, 51, 417
Koesterke, L., Hamann, W.-R., & Gräfener, G. 2002, A&A, 384, 562
Kudritzki, R. P., Puls, J., Lennon, D. J., et al. 1999, A&A, 350, 970
Langer, N. 1989, A&A, 210, 93
Lucy, L. B. 1971, ApJ, 163, 95
Lucy, L. B. & Abbott, D. C. 1993, ApJ, 405, 738
Massey, P. & Johnson, J. 1993, AJ, 105, 980
Nugis, T. & Lamers, H. J. G. L. M. 2002, A&A, 389, 162
Pistinner, S. & Eichler, D. 1995, ApJ, 454, 404
Rauw, G., Vreux, J.-M., Gosset, E., et al. 1996, A&A, 306, 771
Schweickhardt, J., Schmutz, W., Stahl, O., Szeifert, T., & Wolf, B. 1999, A&A, 347, 127
Springmann, U. 1994, A&A, 289, 505
Vink, J. S. & de Koter, A. 2005, A&A, 442, 587
Vink, J. S., de Koter, A., & Lamers, H. J. G. L. M. 1999, A&A, 350, 181